Identification of N-glycan oligomannoside isomers in the diatom Phaeodactylum tricornutum

Rodolphe Dumontier, Corinne Loutelier-Bourhis, Marie-Laure Walet-Balieu, Carole Burel, Alain Mareck, Carlos Afonso, Patrice Lerouge, Muriel Bardor

Carbohydrate Polymers 259 (2021) 117660

Contents lists available at ScienceDirect

Carbohydrate Polymers

journal homepage: www.elsevier.com/locate/carbpol

Identification of *N*-glycan oligomannoside isomers in the diatom *Phaeodactylum tricornutum*

Rodolphe Dumontier [a,b,1], Corinne Loutelier-Bourhis [c,1], Marie-Laure Walet-Balieu [a,b,1], Carole Burel [a,b], Alain Mareck [a,b], Carlos Afonso [c], Patrice Lerouge [a,b,1], Muriel Bardor [a,b,d,1,*]

[a] Normandie University, UNIROUEN, Laboratoire Glycobiologie et Matrice Extracellulaire végétale (Glyco-MEV) EA4358, 76000 Rouen, France
[b] Normandie University, UNIROUEN, SFR NORVEGE, 76000 Rouen, France
[c] Normandie University, UNIROUEN, INSA Rouen, CNRS, UMR6014 - COBRA, 76000 Rouen, France
[d] Univ Lille, CNRS, UMR 8576 - UGSF - Unité de Glycobiologie Structurale et Fonctionnelle, F- 59000 Lille, France

ARTICLE INFO

Keywords:
Glycans
Microalgae
Diatom
Phaeodactylum tricornutum
Oligomannosides
Isomers

ABSTRACT

Microalgae are emerging production systems for recombinant proteins like monoclonal antibodies. In this context, the characterization of the host cell *N*-glycosylation machinery and of the microalgae-made biopharmaceuticals, which are mainly glycoprotein-based products, requires efficient analytical methodologies dedicated to the profiling of the *N*-glycans. Herein, in order to gain knowledge regarding its *N*-glycosylation pathway, we profile the protein *N*-linked oligosaccharides isolated from the diatom *Phaeodactylum tricornutum* that has been used successfully to produce functional monoclonal antibodies. The combination of ion mobility spectrometry–mass Spectrometry and electrospray ionization-multistage tandem mass spectrometry allows us to decipher the detailed structure of the oligomannoside isomers and to demonstrate that the processing of the oligomannosides *N*-linked to proteins occurs in this diatom as reported in mammals. Therefore, *P. tricornutum* synthesizes human-like oligomannosides in contrast to other microalgae species. This represent an advantage as an alternative ecofriendly expression system to produce biopharmaceuticals used for human therapy.

1. Introduction

Nowadays, microalgae are emerging alternative expression systems for the production of biopharmaceuticals (Mathieu-Rivet, Lerouge, & Bardor, 2017; Rosales-Mendoza, 2016; Rosales-Mendoza, Solís-Andrade, Márquez-Escobar, González-Ortega, & Bañuelos-Hernandez, 2020). In this blue biotech context, protein *N*-glycosylation in microalgae is gaining an increasing interest, as most of the biopharmaceuticals are glycoproteins bearing *N*-glycans. Protein *N*-glycosylation is the most common eukaryotic post-translational modifications of secreted proteins (Khoury, Baliban, & Floudas, 2011). It results from the attachment of an oligosaccharide onto the asparagine residues belonging to the consensus sequence Asn-X-Ser/Thr/Cys with X being any amino acid except proline (Burda & Aebi, 1999; Matsui et al., 2011). This process starts in the endoplasmic reticulum (ER) with the biosynthesis of a lipid-linked oligosaccharide (LLO) precursor composed of a $Glc_3Man_9GlcNAc_2$ oligosaccharide linked to a membrane-anchor dolichol pyrophosphate. This LLO is then transferred onto the asparagine residue of the *N*-glycosylation consensus site of the proteins through the action of the oligosaccharyltransferase (Mohorko, Glockshuber, & Aebi, 2011). After this transfer, the glucose residues of the *N*-glycans are removed by α-glucosidases. Trimming of glucose residues together with the interactions between the glycoprotein and ER-resident chaperones ensure the folding and quality control of the glycoprotein (Määttänen, Gehring, Bergeron, & Thomas, 2010). The glycoproteins enter into the Golgi apparatus where $Man_9GlcNAc_2$ (Man-9, Supplemental Figs. 1 and 2) *N*-glycan is then processed through the action of α-mannosidase I activities into a unique canonical $Man_5GlcNAc_2$ (Man-5, Supplemental Fig. 2). Subsequently, a *N*-acetylglucosaminyltransferase I, an α-mannosidase II and a *N*-acetylglucosaminyltransferase II give rise to the *N*-glycan core $GlcNAc_2Man_3GlcNAc_2$, which is common to mammals, insects and land plants (Lerouge et al., 1998; Shi & Jarvis, 2007; Stanley, Taniguchi, & Aebi, 2015). This core undergoes further processing into organism specific complex-type *N*-glycans that

* Corresponding author at: Normandie University, UNIROUEN, Laboratoire Glycobiologie et Matrice Extracellulaire végétale (Glyco-MEV) EA4358, 76000 Rouen, France.
E-mail address: muriel.bardor@univ-rouen.fr (M. Bardor).
[1] Equal contribution of these authors

https://doi.org/10.1016/j.carbpol.2021.117660
Received 4 November 2020; Received in revised form 8 January 2021; Accepted 12 January 2021
Available online 22 January 2021

are involved in multiple essential biological functions (Varki, 2017).

Publications describing the structures of *N*-glycans from different microalgae species have recently revealed that these unicellular organisms synthesize a wide diversity of *N*-glycan structures. Indeed, in addition to oligomannosides, microalgae synthesize mature oligosaccharides consisting of a $Man_2GlcNAc_2$ to $Man_5GlcNAc_2$ core substituted with various pentoses (Xyl*p*, Ara*p*, Ara*f*), hexoses (Gal*p*, Gal*f*, Fuc*p*, GlcNAc*p*) and *O*-methyl groups (Dumontier, Mareck, Mati-Baouche, Lerouge, & Bardor, 2018; Mócsai, Blaukopf, Svehla, Kosma, & Altmann, 2020). With regards to oligomannosides, microalgae synthesize various isomers that rely on the structure of the LLO precursor from which they derived and the specificity of α-mannosidases involved in their trimming. As an example, the green microalga *Chlamydomonas reinhardtii* proteins carry a Man-5 that possess a linear trimannosyl sequence α(1,3)-linked to the β-Man of the core instead of the canonical Man-5 isomer (Vanier et al., 2017). A mixture of Man-5 isomers has also been identified in *Chlorella vulgaris* (Mócsai et al., 2019).

Among the different microalgae species, the diatom *P. tricornutum* appears as one of the most promising expression system investigated so far for the production of biopharmaceuticals. Indeed, functional monoclonal antibodies have been efficiently produced in *P. tricornutum* (Hempel & Maier, 2012; Hempel, Lau, Klingl, & Maier, 2011, 2017; Vanier et al., 2018). Consistently with the *N*-glycan profile identified on total *P. tricornutum* protein extracts (Baïet et al., 2011), the diatom-made monoclonal antibodies carry *N*-linked oligomannosides having 5–9 mannose residues, of which linkages between monomers have not been defined (Vanier et al., 2015). Indeed, *P. tricornutum* oligomannosides may exist as multiple positional isomers depending on the glycosidic linkages between the constitutive α-Man residues. As a consequence, powerful analytical strategies are required for the detailed profiling of the oligomannoside populations. Discrimination between those oligomannoside positional isomers is highly challenging because they are closely related structures and are usually available only in very low amounts. In this context, mass spectrometry appears as a suitable sensitive methodology that allows the structural characterization of oligosaccharide mixtures using tandem mass spectrometry (MS/MS). For instance, multistage tandem mass spectrometry ($ESI\text{-}MS^n$) analyses of *N*-glycans isolated from the bovine ribonuclease B was demonstrated to be able to structurally differentiate the three isomers of Man-7 and Man-8 (Prien, Ashline, Lapadula, Zhang, & Reinhold, 2009) (Supplemental Fig. 2). Since a few years, the coupling of ion mobility spectrometry to mass spectrometry (IMS-MS) allows the separation of oligosaccharide isomers (Harvey et al., 2016; Plasencia, Isailovic, Merenbloom, Mechref, & Clemmer, 2008; Vanier et al., 2017; Lucas et al., 2020; Zhu, Bendiak, Clowers, & Hill, 2009; Zhu, Lee, Valentine, Reilly, & Clemmer, 2012) and the experimental determination of Collision Cross Section (CCS) of ions. These CCS are specific chemical descriptors providing information related to the shape and size of ions in a specific buffer gas. They are used to increase the confidence in structural identification of complex molecules including oligosaccharide isomers (Barroso et al., 2018; Manz & Pagel, 2018; Pagel & Harvey, 2013; Struwe, Pagel, Benesch, Harvey, & Campbell, 2016; Toraño et al., 2020). Herein, we analyzed the detailed structures of the oligomannosides ranging from Man-5 to Man-9 isolated from *P. tricornutum* endogenous proteins by a combination of IMS-MS and $ESI\text{-}MS^n$. The results allow gaining knowledge regarding the *N*-glycosylation capacity of *P. tricornutum* that is currently developed as a green cell biofactory for the production of biopharmaceuticals, especially monoclonal antibodies intended to be used for human immunotherapy.

2. Materials and methods

2.1. Materials

P. tricornutum (Pt 1.8.6) was grown and collected as reported previously (Baïet et al., 2011). Bovine ribonuclease B and peptide *N*-glycosidase F (PNGase F) were purchased from Sigma (R7884) and Roche (NGLY-R0), respectively. All buffers, solvents and reagents used were Liquid Chromatography (LC) – Mass Spectrometry (MS) grade.

2.2. Methods

2.2.1. N-glycans preparation

P. tricornutum cell pellet was recovered by centrifugation at 4,500 g during 5 min at 19 °C. Total proteins from *P. tricornutum* were extracted as previously described in (Zhang et al., 2019) using a Tris 0.1 M pH 7.5 buffer containing a tablet of SIGMA*FAST*™ Protease Inhibitor Cocktail, EDTA-Free (SIGMA). Then, the protein extract was spun down during 30 min at 15,000 *g*. The supernatant was dialyzed (6,000–8,000 Da molecular cut off, Fisher Chemical) for 24 h against deionised water. Then, 10 mg of proteins from *P. tricornutum* were freeze dried prior to enzymatic deglycosylation using the PNGase F as previously reported (Baïet et al., 2011). Briefly, proteins were resuspended in 1 mL of Tris 0.1 M pH 7.5 buffer containing 0.1 % of SDS (w/v). Samples were heated at 100 °C during 10 min. After cooling down, one mL of Tris 0.1 M pH 7.5 buffer containing 0.5 % d'IGEPAL® (v/v) (MP bio, CA-630) was added prior to 15 units of PNGase F. Samples were then incubated overnight at 37 °C under agitation. One mg of bovine ribonuclease B was digested and treated in parallel to the *P. tricornutum* samples. Subsequently, deglycosylated proteins were precipitated with 4 volumes of ethanol at −20 °C during 24 h. Samples were centrifuged at 20,000 *g* for 15 min. The supernatants containing the released *N*-glycans were air-dried. *N*-glycans from *C. reinhardtii* were prepared as previously reported (Lucas et al., 2020).

2.2.2. N-glycans derivatization

The free *N*-glycans were labelled with 2-aminobenzamide (2AB) according to the literature (Vanier et al., 2017). Briefly, 10 mg of 2AB suspended in 200 µL of acetic acid/anhydrous DMSO (SIGMA) (70/30, v/v) were mixed with 12 mg of sodium cyanoborohydride. Ten µL of this mixture were added on the dried *N*-glycans. Samples were then incubated at 60 °C during 2 h. Excess of reagent was removed using a cartridge D1 from Ludger according to the manufacturer's instructions. Permethylation of samples was performed as described (Ciucanu & Kerek, 1984). Permethylated 2AB labelled *N*-glycans were clean-up using 3 mL C18 columns (Hypersep C18, Thermo Fisher) as reported in Vanier et al. (2017). Permethylated *N*-glycans retained on the C18 stationary phase were eluted subsequently using 2 mL of 15 % acetonitrile, 35 % acetonitrile, 50 % and finally 75 % of acetonitrile. The fraction eluted with 50 % acetonitrile was air-dried prior to mass spectrometry analysis.

2.2.3. Ion mobility spectrometry – mass spectrometry (IMS-MS)

The IMS-MS experiments were performed using a Waters SYNAPT G2 hybrid quadrupole/time of flight instrument equipped with an ESI LockSpray™ source, (Waters, Manchester, UK). The SYNAPT HDMS system was calibrated using sodium formate cluster ions (2 $mg.mL^{-1}$) and operated in 'V' resolution mode (resolution 20,000 FWHM for full width at half maximum). The ESI parameters were in positive ion mode: capillary voltage 3.1 kV; sample cone voltage 70 V; source temperature, 90 °C; desolvation temperature, 300 °C; desolvation gas flow (N_2), 700 $L.h^{-1}$. The data were acquired using a 50-2,000 *m/z* range with 1 s scan time and 0.02 s interscan delay. Sample solutions were infused into the source at 400 $\mu L.h^{-1}$ with a syringe pump (Cole-Palmer, Vernon Hills, Illinois, USA). The IMS conditions were: gas flow (N_2), 90 $mL.min^{-1}$; IMS cell pressure, 2.98 mbar; IMS traveling wave height voltage, 40 V and T-wave velocity, 550 $m.s^{-1}$ for 2AB glycans and 700 ms^{-1} for permethylated 2AB derivatives. Helium gas flow was 180 $mL.min^{-1}$. IMS wave delay was 450 µs. Data were recorded from three independent preparations and processed using the Mass Lynx 4.1 and the Drift Scope 2.2 softwares (Waters, Manchester, UK).

Collision Cross Section (CCS, Ω) of oligomannosides were deter-

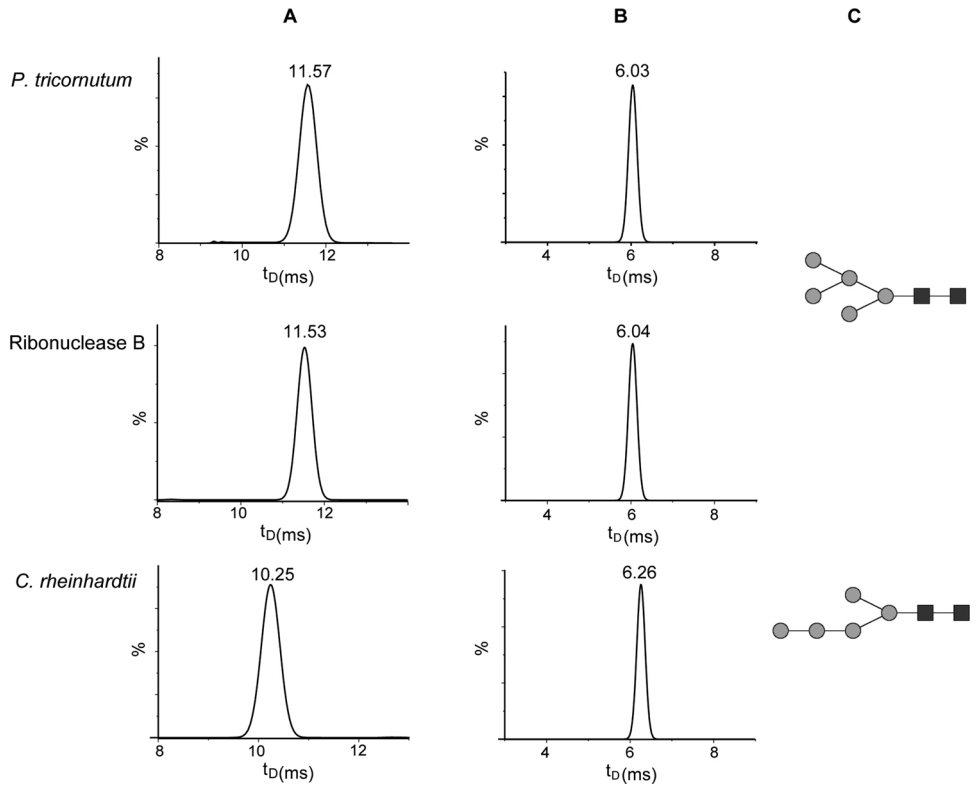

Fig. 1. Drift time (t_D) recorded by Ion Mobility Spectrometry–Mass Spectrometry (IMS-MS) of non-permethylated (A) and permethylated (B) 2AB Man-5 isolated from *P. tricornutum*, bovine ribonuclease B and *C. reinhardtii* proteins. (C) Structures of the canonical (middle) Man-5 *N*-linked to bovine ribonuclease B and the non-canonical Man-5 as described in *C. reinhardtii* (bottom), respectively. Grey square: *N*-acetylglucosamine, grey circle: Mannose.

mined according to the literature data (Smith et al., 2009). Depending on their charge, shape and size (related to Ω), the ion migrates at different velocities and pass through the IMS cell at different drift times (t_d). The ion velocity (v) is related to the ion mobility (K) by Eq. (1):

$$K = \frac{v}{E} = \frac{L}{t_d\ E} \tag{1}$$

where E is the electric field and L the length of the IM cell. The ion mobility K is also related to Ω in a define buffer gas according to Eq. (2) (Revercomb & Mason, 1975):

$$K = \frac{3ze}{16N} \times \sqrt{\left(\frac{1}{m} + \frac{1}{M}\right)} \times \sqrt{\frac{2\pi}{k_b T}} \times \frac{T}{273.15} \frac{760}{P} \times \frac{1}{\Omega} \tag{2}$$

where ze is the ion charge, m and M are respectively the mass of the ion and of the buffer gas, k_b is the Boltzmann constant, N, P and T are the number density, the pressure and the temperature of the buffer gas. Thus, in uniform electric field (drift tube ion mobility, DTIMS), the CCS can be determined directly from the drift time t_d, according to the Mason-Schamp Eq. (3) (Revercomb & Mason, 1975):

$$\Omega = \frac{3ze}{16N} \times \sqrt{\left(\frac{1}{m} + \frac{1}{M}\right)} \times \sqrt{\frac{2\pi}{k_b T}} \times \frac{T}{273.15} \frac{760}{P} \times \frac{t_d\ E}{L} \tag{3}$$

In TWIMS cells, the electric field is not constant and uniform. The Eq. (3) is not applicable and the relation between t_d and Ω is then expressed by the Eq. (4) (Smith et al., 2009):

$$\Omega = \frac{3ze}{16N} \times \sqrt{\left(\frac{1}{m} + \frac{1}{M}\right)} \times \sqrt{\frac{2\pi}{k_b T}} \times \frac{760}{P} \times \frac{T}{273,15} \times At_d{}^B \tag{4}$$

where A and B are the correction factors related to the electric field E and to the compensation of the non-linearity of E, respectively (Wildgoose et al., 2006). This relation can be simplified to Eq. (5):

$$\Omega' = A' t_d{}^B \tag{5}$$

where $A' = \frac{3}{16N} \times \sqrt{\frac{2\pi}{kT}} \times \frac{760}{P} \times \frac{T}{273.15} \times A$

and $\Omega' = \frac{\Omega}{ze\sqrt{\left(\frac{1}{m}+\frac{1}{M}\right)}} = \frac{\Omega}{ze\sqrt{1/\mu}}$

To obtain CCS of an analyte ion, the coefficients A' and B need to be determined *via* the calibration of the TWIMS cell using reference compounds of known CCS. These reference ions must exhibit the same charge state as analyte ions. Various calibrating substances are available which CCS have been reported either in helium or in nitrogen (Bush, Campuzano, & Robinson, 2012; Pagel & Harvey, 2013). Note that experimental CCS determined with a TWIMS cell can be labelled as ^{TW}CCS, and more precisely as $^{TW}CCS_{N2\rightarrow He}$ when estimated in helium and as $^{TW}CCS_{N2\rightarrow N2}$ when estimated in nitrogen as recommended (May, Morris, & McLean, 2017)

Correlating measured drift time (t_d) of calibrant ions with corresponding reduced CCS Ω' according to Smith et al. (2009) method permit to plot a calibration curve: $\text{Ln}\ \Omega' = \text{LnA}' + \text{B Ln}\ t_d$. In our case, two sets of TWIMS cell calibration were performed, the first to determine ^{TW}CCS of non-permethylated 2AB labelled *N*-glycans for which $[M + Na]^+$ adducts of dextran were used, the second to determine ^{TW}CCS of permethylated 2AB derivatives for which $[M+2Na]^{2+}$ ions of dextran were applied. The experimental values for ^{TW}CCS were measured with a relative error below 2% as reported in the literature (Hines, May, McLean, & Xu, 2016). The drift times of both sample and reference ions were accurately determined by fitting the extracted ion mobility spectra with a Gaussian regression (OriginPro 2016 b9.3.226 software, OriginLab).

Table 1
Experimental Collision Cross Section (CCS; $^{TW}CCS_{N2\rightarrow N2}$) determined for permethylated 2AB derivatives of Man-5 to Man-9 oligomannosides isolated from *P. tricornutum* proteins and from the bovine ribonuclease B.

Permethylated 2AB derivatives	$[M+2Na]^{2+}$ (*m/z*)	Ω_{N2} (Å^2)	
		Ribonuclease B	*P. tricornutum*
Man-5	882.5	**455.9**	**455.6**
Man-6	984.6	**494.0**	**492.8**
Man-7	1086.7	**528.9**	**527.7**
Man-8	1188.7	**561.0**	**560.0**
Man-9	1290.8	**595.0**	**591.2**

2.2.4. Multistage tandem mass spectrometry analysis

Permethylated 2AB *N*-glycans were analyzed by ESI-MS^n (n = 2-4) using a Bruker HCT Ultra ETD II quadrupole ion trap (QIT) mass spectrometer and the data were processed using the Esquire Control 6.2 and Data Analysis 4.0 softwares (Bruker Daltonics, Bremen, Germany). The ESI parameters, in positive ion mode, were as followed: capillary voltage set at −3.5 kV, end plate offset at −500 V, skimmer and capillary exit voltages set at 40 V and 200 V, respectively, nebulizer gas (N_2), pressure, drying gas (N_2) flow rate and drying gas temperature were 10 psi, 7.0 L.min^{-1} and 300 °C, respectively. Helium pressure in the ion trap was 1.3 × 10^{-5} mbar. The data were acquired using a 200-2200 *m/z* range, using a scan speed of 8100 *m/z* per second. The number of ions entering the trap cell was automatically adjusted by controlling the accumulation time using the ion charge control (ICC) mode (target 100,000) with a maximum accumulation time of 50 ms. The injection low-mass cut-off (LMCO) value was *m/z* 120. The values of spectrum averages and rolling average were 6 and 2. ESI-MS^n experiments were carried out by Collision Induced Dissociation (CID) using helium as the collision gas, isolation width of 1 *m/z* unit for the precursor ions and 2 *m/z* unit for the intermediate ions using a resonant excitation frequency with an amplitude from 0.8 to 0.9 Vp–p. Samples were dissolved in 100 µL of CH_3OH/H_2O 1/1 v/v and then diluted twice or 100-fold in the same solvent system for *P. tricornutum* and ribonuclease B, respectively. The final solutions were infused into the source at a flow rate of 180 µL.h^{-1} by means of a syringe pump (Cole-Palmer, Vernon Hills, IL, USA). External calibration was performed using the 'tuning mix' from Agilent Technologies (Santa Rosa, CA, USA). All mass spectra were manually interpreted according to the literature (Domon & Costello, 1988; Prien et al., 2009). The Glycoworkbench software v2.1 was used to confirm the assignment of the fragment ions.

3. Results and discussion

3.1. Analysis by IMS-MS and ESI-MS^n of *P. tricornutum* Man-5 oligomannoside

2-aminobenzamide (2AB) labelled *N*-glycans from *P. tricornutum* proteins were divided in two fractions, one being permethylated. The 2AB derivatives of the diatom Man-5 oligomannoside was first analyzed by IMS-MS. The ion mobility peak of the $[M + Na]^+$ adduct of 2AB labelled Man-5 was compared to the ion mobility peaks of 2AB derivatives of two Man-5 used herein as references; the canonical Man-5 isolated from the bovine ribonuclease B (Fig.1C; Fu, Chen, & O'Neill, 1994) and the non-canonical 2AB Man-5 prepared from *C. reinhardtii* proteins that contains a linear trimannosyl sequence linked to C3 of the β-Man (Fig. 1C; Vanier et al., 2017). The canonical 2AB Man-5 from bovine ribonuclease B and the Man-5 derivative from *P. tricornutum* proteins exhibited drift times t_D of 11.53 and 11.57 ms respectively, which is within the experimental error. This suggests that they share the same structure. In contrast, non-canonical 2AB Man-5 from *C. reinhardtii* exhibited a t_D of 10.25 ms (Fig. 1A). Similar results were observed when the analysis by IMS-MS was performed on $[M+2Na]^{2+}$ adducts of permethylated 2AB Man-5 derivative from *P. tricornutum* as compared to the canonical permethylated 2AB Man-5 isolated from the bovine ribonuclease B and the non-canonical permethylated 2AB Man-5 structures from *C. reinhardtii* (Fig. 1B). Experimental CCS values of permethylated 2AB Man-5 were then determined by IMS-MS using dextran oligomers as

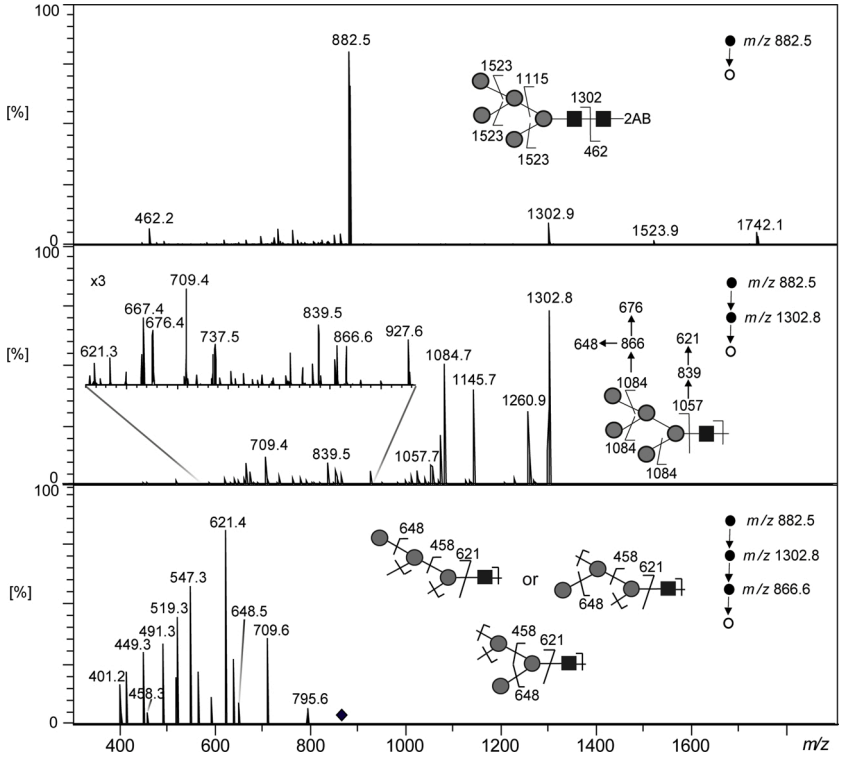

Fig. 2. Fragmentation pattern for *m/z* 882.5 $[M+2Na]^{2+}$ precursor ion and multistage tandem mass spectra (n = 2, 3 and 4) of permethylated 2AB Man-5 derivative isolated from *P. tricornutum* proteins. Grey square: *N*-acetylglucosamine, grey circle: Mannose.

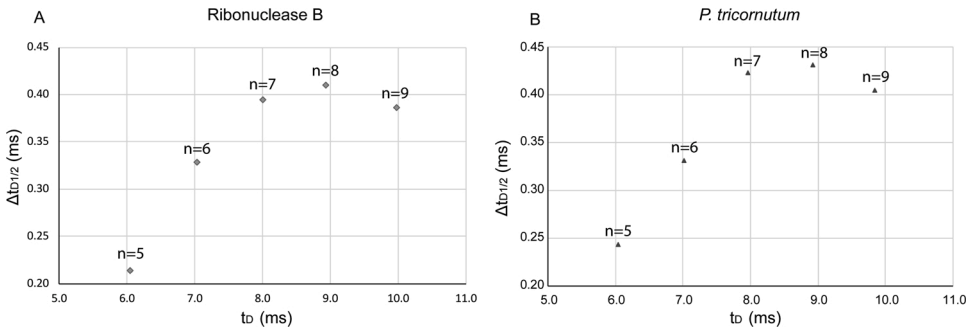

Fig. 3. Full width at half maximum (FWHM, $\Delta t_{D1/2}$) according to the drift time (t_D) for permethylated 2AB Man-5 to Man-9 isolated from (A) bovine ribonuclease B and (B) *P. tricornutum*. n: number of mannose residues.

calibrants and and their CCS previously published in either nitrogen or helium buffer gas (Hoffmann, Hofmann, & Pagel, 2014) (Table 1 and Supplemental Table 1).

Data recorded by IMS-MS suggested that *P. tricornutum* proteins carry a unique canonical Man-5 isomer. For confirmation, the structure of *P. tricornutum* Man-5 isomer was further investigated by ESI-MS^n with n = 2, n = 3 and n = 4. ESI-MS^n of the doubly charged $[M+2Na]^{2+}$ ion of permethylated 2AB Man-5 (*m/z* 882.5) from *P. tricornutum* revealed a fragmentation pattern *m/z* 882.5 → *m/z* 1302.8 → *m/z* 1084.7 → *m/z* 866.6 → *m/z* 648.5 that is consistent with the canonical isomer of permethylated 2AB Man-5 (Fig. 2). Similar pattern of fragmentation was observed for $[M+2Na]^{2+}$ precursor ion of permethylated 2AB Man-5 obtained from bovine ribonuclease B (Supplemental Fig. 3) and differed from the ESI-MS^n fragmentation pattern of the permethylated 2AB Man-5 obtained from *C. reinhardtii* proteins (Vanier et al., 2017). Taken together, IMS-MS data as well as ESI-MS^n fragmentation patterns

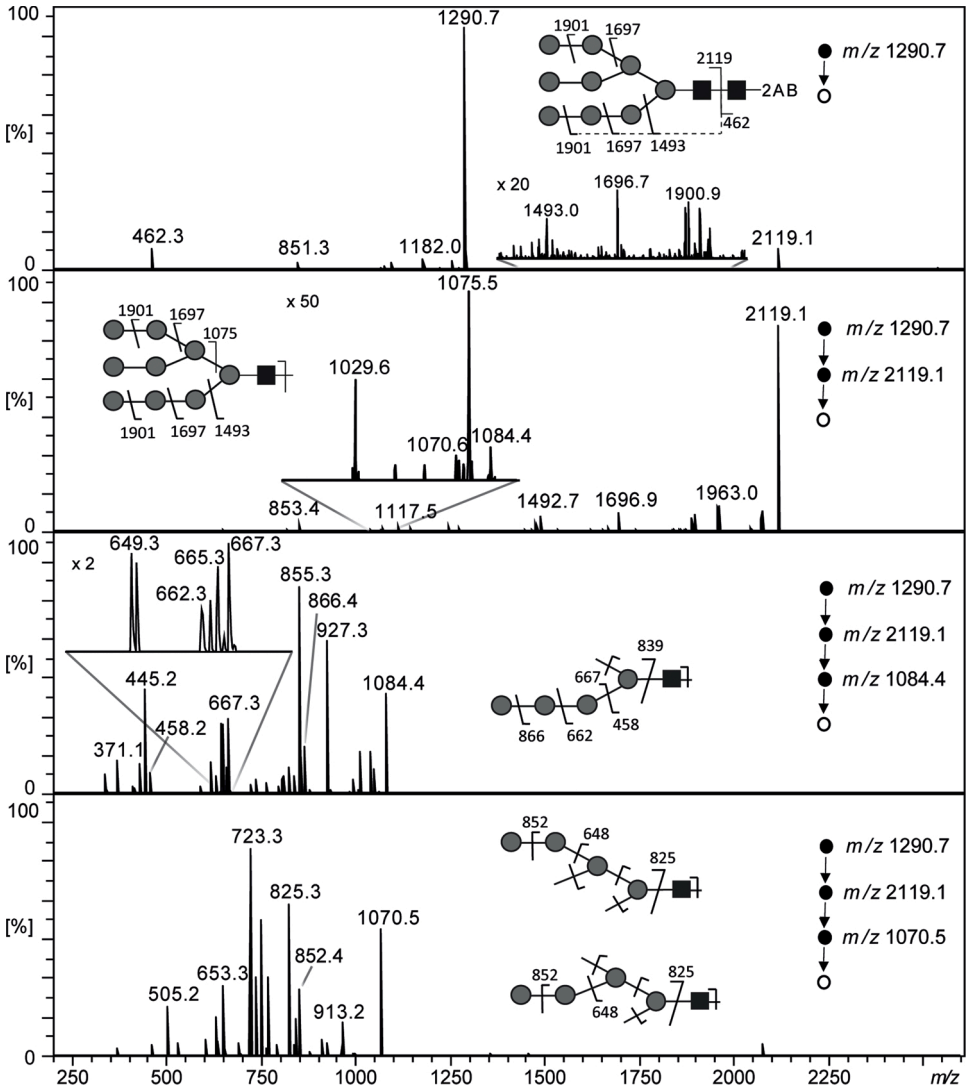

Fig. 4. Fragmentation pattern for *m/z* 1290.7 $[M+2Na]^{2+}$ precursor ion and multistage tandem mass spectra (n = 2, 3 and 4) of permethylated 2AB Man-9 derivative isolated from *P. tricornutum* proteins. Grey square: *N*-acetylglucosamine, grey circle: Mannose.

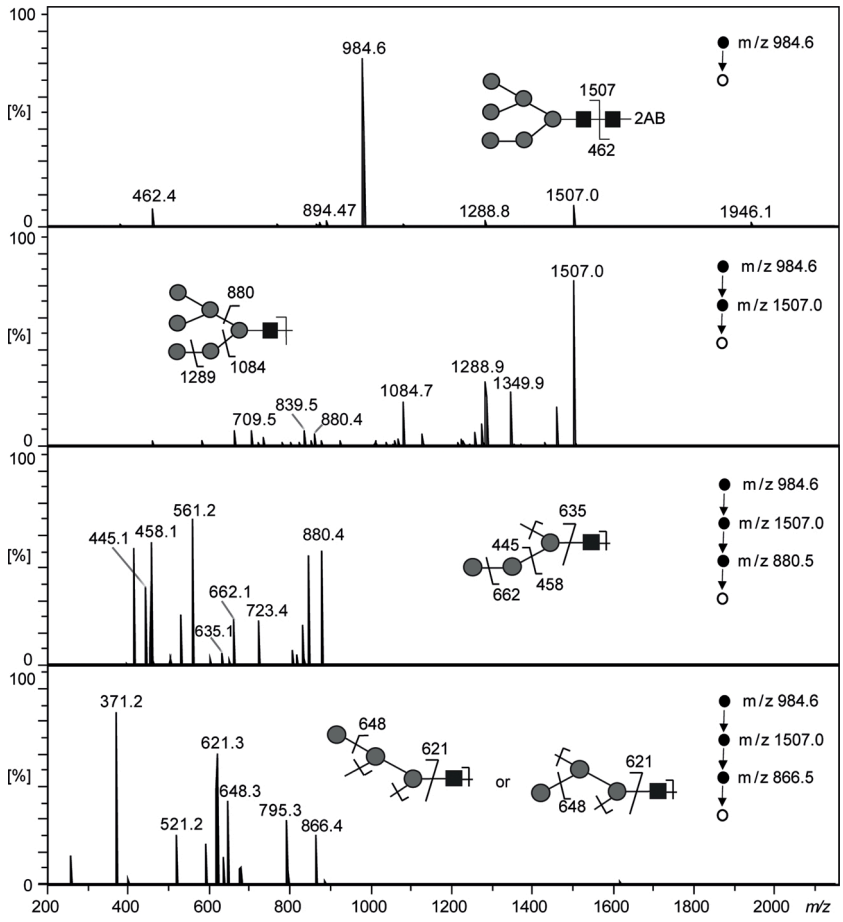

Fig. 5. Fragmentation pattern for *m/z* 984.6 $[M+2Na]^{2+}$ precursor ion and multistage tandem mass spectra (n = 2, 3 and 4) of permethylated 2AB Man-6 derivative isolated from *P. tricornutum* proteins. Grey square: *N*-acetylglucosamine, grey circle: Mannose.

demonstrated that *P. tricornutum* proteins carry a unique canonical Man-5 oligomannoside as reported in the literature for mammal, insect and plant cells (Lerouge et al., 1998; Shi & Jarvis, 2007; Stanley et al., 2015).

3.2. Analysis by IMS-MS of P. tricornutum oligomannosides

The structural analysis of *P. tricornutum* oligomannosides was extended to the other oligomannosides going from Man-6 to Man-9. Analysis of the whole diatom *N*-glycan population was investigated by IMS-MS taking advantage of data recorded for Man-6 to Man-9 oligomannosides isolated from bovine ribonuclease B for which structures of each isomer have been already reported. Indeed, bovine ribonuclease B is *N*-glycosylated by unique isomers of Man-5, Man-6 and Man-9 respectively, whereas different positional isomers of Man-7 and Man-8 have been structurally characterized by proton NMR (Fu et al., 1994), mass spectrometry coupled to liquid chromatography (Costello, Contado-Miller, & Cipollo, 2007) and ESI-MS^n (Prien et al., 2009) (Supplemental Fig. 2). The experimental CCS determined by IMS-MS using nitrogen as buffer gas showed that values from *P. tricornutum* oligomannosides were very close to those from bovine ribonuclease B oligomannosides suggesting that both oligomannoside populations are closely related (Table 1). Similar observation and conclusion can be drawn from experimental CCS recorded in helium as buffer gas (Supplemental Table 1).

The presence of positional isomers for each oligomannoside was investigated by measuring the ion mobility peak width (full width at half maximum, FWHM) that has been recently reported as an isomeric descriptor (Farenc et al., 2017; Mendes Siqueira et al., 2018). The presence of unresolved isomers can be detected based on the ion mobility peak broadening. FWHM for permethylated 2AB Man-5 to Man-9 ion mobility peaks were determined according to the method previously described for other classes of compounds (Fig. 3; Farenc et al., 2017; Mendes Siqueira et al., 2018). In the case of Man-5 and Man-9 that present only one isomer in view of the NMR data, the FWHM should be related only to the diffusion phenomenon. As shown previously, this factor rise almost linearly with the drift time (Farenc et al., 2017).

The plots of FWHM ($\Delta t_{D1/2}$) values in function of drift time t_D for permethylated 2AB derivatives of bovine ribonuclease B oligomannosides present higher values of FWHM than expected for Man-6, Man-7 and Man-8 (Fig. 3A). Thus, in contrast to Man-5 and Man-9 that both exist as unique isomer (smaller $\Delta t_{D1/2}$), the higher $\Delta t_{D1/2}$ observed for Man-6, Man-7 and Man-8 is likely due to the presence of positional isomers for these oligomannosides. Similar trend has been observed for *P. tricornutum* (Fig. 3B).

3.3. Structural analysis by ESI-MS^n of P. tricornutum Man-6 to Man-9 oligomannosides

The structures of *P. tricornutum* oligomannosides were further investigated by ESI-MS^n analysis of the doubly charged $[M+2Na]^{2+}$ ions of permethylated samples in order to determine the different positional isomers and their respective structures by comparison of ESI-MS^n fragmentation patterns with those of oligomannosides isolated from the bovine ribonuclease B (Prien et al., 2009).

In agreement with the CCS (Table 1) and FWHM measurements (Fig. 3), ESI-MS^n fragmentation pattern of $[M+2Na]^{2+}$ ion of

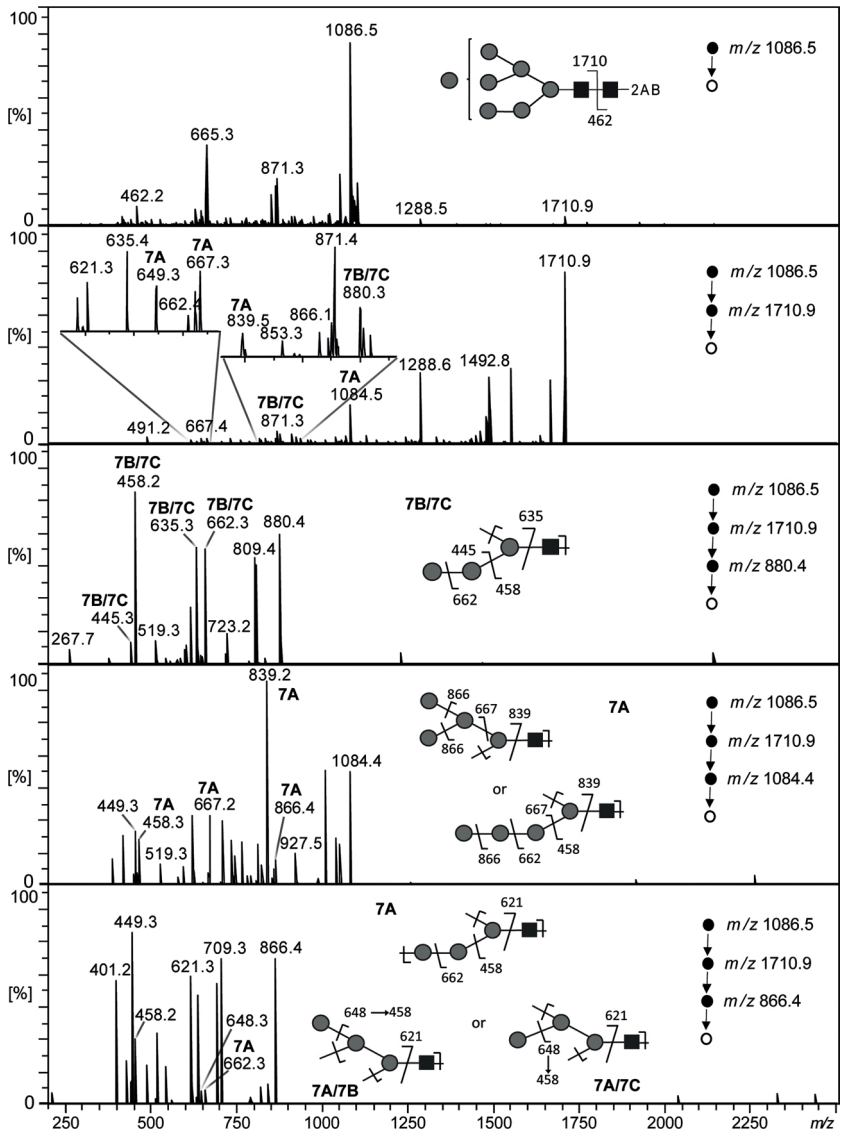

Fig. 6. Fragmentation pattern for *m/z* 1086.5 $[M+2Na]^{2+}$ precursor ion and multistage tandem mass spectra (n = 2, 3 and 4) of mixture of permethylated 2AB Man-7 derivative isolated from *P. tricornutum* proteins. Grey square: *N*-acetylglucosamine, grey circle: Mannose.

permethylated Man-9 isolated from *P. tricornutum* proteins (Fig. 4) indicated that this oligomannoside exists as a unique isomer that is identical to the Man-9 of the bovine ribonuclease B (Supplemental Fig. 4) (Prien et al., 2009). With regards to Man-6, ESI-MS^n pattern of the doubly charged $[M+2Na]^{2+}$ ions at *m/z* 984.6 from *P. tricornutum* proteins (Fig. 5) and bovine ribonuclease B (Supplemental Fig. 5) revealed similar fragmentation patterns *m/z* 984.6 → *m/z* 1507.0 → *m/z* 880.4 (or → *m/z* 866.4) specific for the Man-6 isomer represented in Supplemental Fig. 2. No other positional isomer was detected in the MS spectra of the Man-6 isolated from *P. tricornutum* proteins, although the presence of minor isomers cannot be ruled out because of the observed weak peak broadening for Man-6 (Fig. 3).

The analyses of the ESI-MS^n fragmentation patterns of the doubly charged $[M+2Na]^{2+}$ ions of permethylated 2AB derivatives of Man-7 (*m/z* 1086.5) and Man-8 (*m/z* 1188.6) suggest that these oligomannosides exist as a mixture of positional isomers. As illustration, the main Man-7 fragmentation pattern *m/z* 1086.5 → *m/z* 1710.9 → *m/z* 880.4 → *m/z* 662.3 → *m/z* 458.2 is specific for Man-7B and Man-7C, whereas the successive fragmentations *m/z* 1086.5 → *m/z* 1710.9 → *m/z* 1084.4 → *m/z* 839.2 → *m/z* 648.3 are specific for the Man-7A isomer (Fig. 6, Supplemental Schemes 1 and 2). For Man-8, the fragmentation pattern *m/z* 1188.6 → *m/z* 1915.0 → *m/z* 1084.5 → *m/z* 866.4 → *m/z* 662.3 is consistent with the Man-8B and C isomers having a linear trimannosyl sequence located on the β-Man, whereas the sequence of fragmentation *m/z* 1188.6 → *m/z* 1915.0 → *m/z* 880.4 → *m/z* 662.3 → *m/z* 458.2 is discriminant for a Man-8A isomer (Fig. 7, Supplemental Schemes 3 and 4). Similar fragmentation patterns were observed for Man-7 and Man-8 mixture of positional isomers isolated from bovine ribonuclease B (Supplemental Figs. 6 and 7; Prien et al., 2009).

These data demonstrated that proteins from *P. tricornutum* are *N*-glycosylated with single isomers of Man-5, Man-6 and Man-9 oligomannosides and mixtures of isomers of Man-7 and Man-8 (Fig. 8).

4. Conclusion

In conclusion, in this work, structures of oligomannosides isolated from *P. tricornutum* proteins were investigated by IMS-MS and ESI-MS^n using glycans *N*-linked to bovine ribonuclease B and proteins of *C. reinhardtii* as references. The structural analysis of Man-5 from *P. tricornutum* proteins clearly demonstrated that this diatom synthesizes a unique canonical Man-5 isomer as observed in mammals (Fig. 8). This result is consistent with the expression in *P. tricornutum* of a *N*-

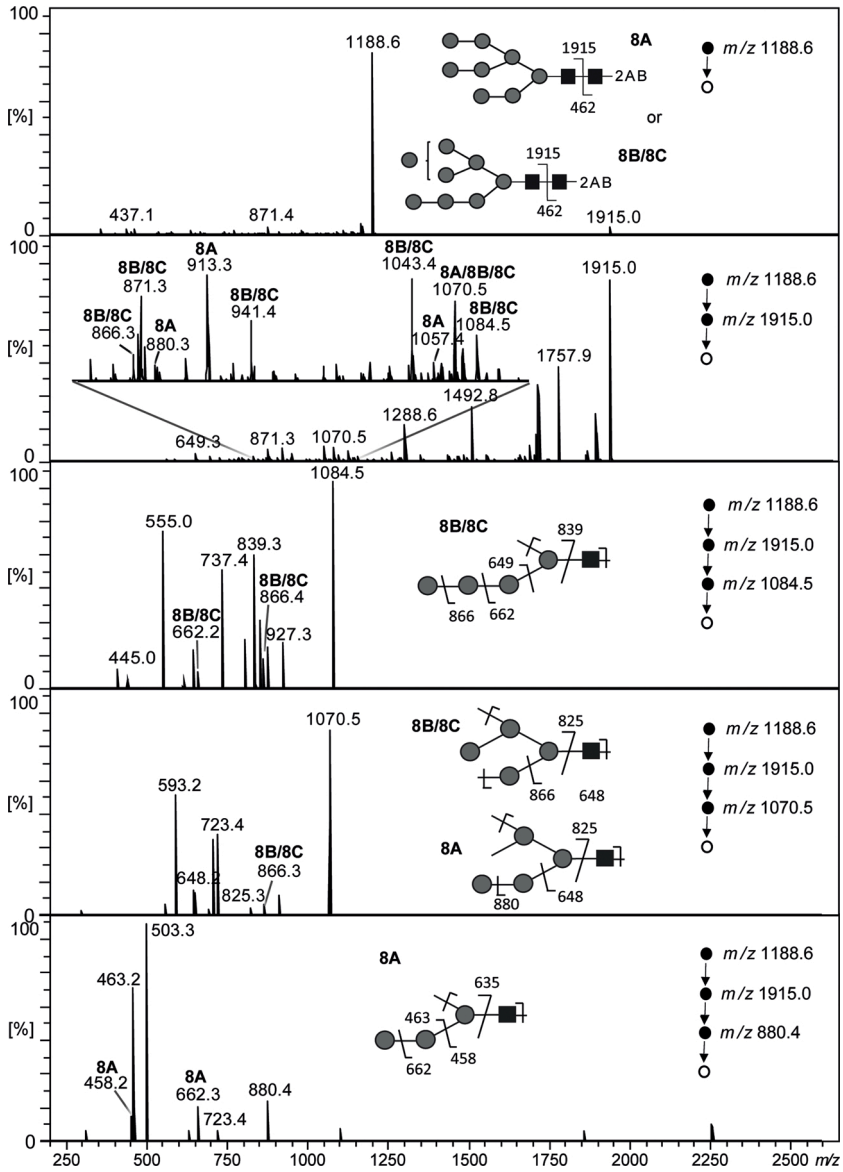

Fig. 7. Fragmentation pattern for *m/z* 1188.6 $[M+2Na]^{2+}$ precursor ion and multistage tandem mass spectra (n = 2, 3 and 4) of mixture of permethylated 2AB Man-8 isolated from *P. tricornutum* proteins. Grey square: *N*-acetylglucosamine, grey circle: Mannose.

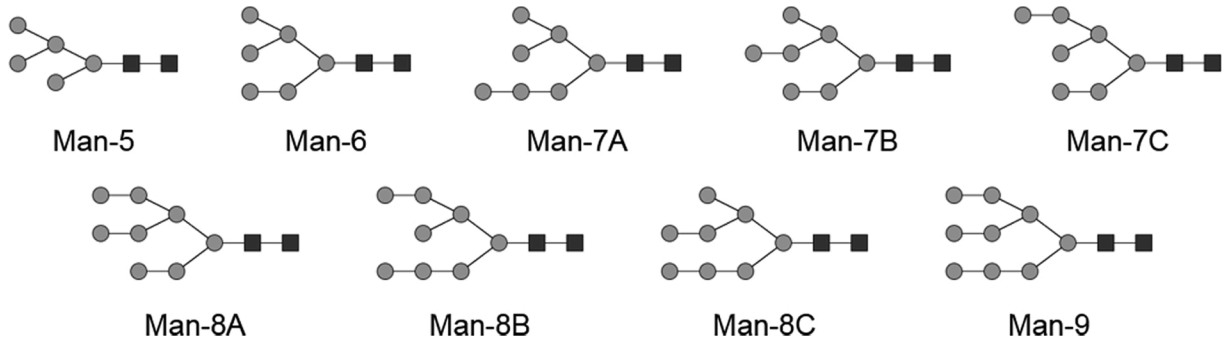

Fig. 8. Structures of main oligomannoside isomers isolated from *P. tricornutum* proteins. Grey square: *N*-acetylglucosamine, grey circle: Mannose.

acetylglucosaminyltransferase I that is supposed to transfer a terminal GlcNAc residue specifically on this canonical Man-5 (Baïet et al., 2011; Zhang et al., 2019). This suggests that this diatom is able to initiate the processing of oligomannosides into complex type *N*-glycans although only trace amounts of mature *N*-glycans have only been detected (Baïet et al., 2011; Zhang et al., 2019). This study also demonstrated that oligomannosides Man-6 and Man-9 *N*-linked to *P. tricornutum* proteins exist as unique isomers, although the presence of minor Man-6 isomers cannot be completely ruled out. In contrast, Man-7 and Man-8 exist as different positional isomers as observed for the oligomannosides

isolated from bovine ribonuclease B (Supplemental Fig. 2).

Since the structures of *P. tricornutum* oligomannosides are identical to those of the bovine ribonuclease B, we conclude that the trimming of the glycan precursor in the Golgi apparatus by α-mannosidases occurs as reported in mammals and give rise to the unique canonical Man-5. These data further support *P. tricornutum* as a suitable system for the engineering of its endogenous glycan machinery for the production of therapeutic proteins carrying human-like *N*-glycans. Moreover, if the production of therapeutic proteins *N*-glycosylated with oligomannosides, such as lysosomal enzymes, is envisioned, their expression in *P. tricornutum* would result in recombinant proteins harboring an optimal *N*-glycosylation.

Author contributions

R.D., C.L.-B., M.-L.W.-B., C.B. performed the experimental work; R. D., M.-L.W.-B., C.L.-B., M.B., P.L. analyzed the data; M.B. and P.L. conceptualized and coordinated the work. The manuscript was written through contributions of all authors. All authors have given approval to the final version of the manuscript.

Acknowledgements

The authors are grateful for generous and financial support from theEuropean Union's Horizon 2020 Research and Innovation programme under the Grant Agreement 774078 (Pharma-Factory); the IUF (Institut Universitaire de France, 2014-2019); the Normandie Université (NU), the Centre National de la Recherche Scientifique (CNRS), Université de Rouen Normandie (URN), INSA Rouen Normandie; the European Regional Development Fund (ERDF) N° HN0001343, the Région Normandie, and the Laboratoire d'Excellence (LabEx) SynOrg (ANR-11-LABX-0029), France. M.L.W.B. fellowship is supported by the European Union's Horizon 2020 Research and Innovation programme under the Grant Agreement 774078 (Pharma-Factory).

Appendix A. Supplementary data

Supplementary material related to this article can be found, in the online version, at doi:https://doi.org/10.1016/j.carbpol.2021.117660.

References

Baïet, B., Burel, C., Saint-Jean, B., Louvet, R., Menu-Bouaouiche, L., Kiefer-Meyer, M.-C., et al. (2011). *N*-glycans of *Phaeodactylum Tricornutum* diatom and functional characterization of Its *N*-acetylglucosaminyltransferase I enzyme. *The Journal of Biological Chemistry, 286*(8), 6152–6164.

Barroso, A., Giménez, E., Konijnenberg, A., Sancho, J., Sanz-Nebot, V., & Sobott, F. (2018). Evaluation of ion mobility for the separation of glycoconjugate isomers due to different types of sialic acid linkage, at the intact glycoprotein, glycopeptide and glycan level. *Journal of Proteomics, 173*, 22–31.

Burda, P., & Aebi, M. (1999). The dolichol pathway of N-linked glycosylation. *Biochimica et Biophysica Acta, 1426*(2), 239–257.

Bush, M. F., Campuzano, I. D. G., & Robinson, C. V. (2012). Ion mobility mass spectrometry of peptide ions: Effects of drift gas and calibration strategies. *Analytical Chemistry, 84*(16), 7124–7130.

Ciucanu, I., & Kerek, F. (1984). A simple and rapid method for the permethylation of carbohydrates. *Carbohydrate Research, 131*(2), 209–217.

Costello, C. E., Contado-Miller, J. M., & Cipollo, J. F. (2007). A glycomics platform for the analysis of permethylated oligosaccharide alditols. *Journal of the American Society for Mass Spectrometry, 18*(10), 1799–1812.

Domon, B., & Costello, C. E. (1988). A systematic nomenclature for carbohydrate fragmentations in FAB-MS/MS spectra of glycoconjugates. *Glycoconjugate Journal, 5*(4), 397–409.

Dumontier, R., Mareck, A., Mati-Baouche, N., Lerouge, P., & Bardor, M. (2018). Toward future engineering of the *N*-glycosylation pathways in microalgae for optimizing the production of biopharmaceuticals. In E. Jacob-Lopes, L. Queiroz Zepka, & I. Queiroz (Eds.), *Microalgal biotechnology* (pp. 177–193).

Farenc, M., Paupy, B., Marceau, S., Riches, E., Afonso, C., & Giusti, P. (2017). Effective ion mobility peak width as a new isomeric descriptor for the untargeted analysis of complex mixtures using ion mobility-mass spectrometry. *Journal of the American Society for Mass Spectrometry, 28*(11), 2476–2482.

Fu, D., Chen, L., & O'Neill, R. A. (1994). A detailed structural characterization of ribonuclease B oligosaccharides by 1H NMR spectroscopy and mass spectrometry. *Carbohydrydrate Research, 261*(2), 173–186.

Harvey, D. J., Scarff, C. A., Edgeworth, M., Struwe, W. B., Pagel, K., Thalassinos, K., et al. (2016). Travelling-wave ion mobility and negative ion fragmentation of high-mannose *N*-glycans. *Journal of Mass Spectrometry, 51*(3), 219–235.

Hempel, F., & Maier, U. G. (2012). An engineered diatom acting like a plasma cell secreting human IgG antibodies with high efficiency. *Microbial Cell Factories, 11*(1), 126.

Hempel, F., Lau, J., Klingl, A., & Maier, U. G. (2011). Algae as protein factories: Expression of a human antibody and the respective antigen in the diatom *Phaeodactylum tricornutum*. *PloS One, 6*(12).

Hempel, F., Maurer, M., Brockmann, B., Mayer, C., Biedenkopf, N., Kelterbaum, A., et al. (2017). From hybridomas to a robust microalgal-based production platform: Molecular design of a diatom secreting monoclonal antibodies directed against the Marburg virus nucleoprotein. *Microbiolial Cell Factories, 16*(1), 131.

Hines, K. M., May, J. C., McLean, J. A., & Xu, L. (2016). Evaluation of collision cross section calibrants for structural analysis of lipids by traveling wave ion mobility-mass spectrometry. *Analytical Chemistry, 88*(14), 7329–7336, 2016.

Hoffmann, W., Hofmann, J., & Pagel, K. (2014). Energy-resolved ion mobility-mass spectrometry: A concept to improve the separation of isomeric carbohydrates. *Journal of the American Society for Mass Spectrometry, 25*(3), 471–479.

Khoury, G. A., Baliban, R. C., & Floudas, C. A. (2011). Proteome-wide post-translational modification statistics: frequency analysis and curation of the Swiss-prot database. *Scientific Reports, 1*(1), 1–5.

Lerouge, P., Cabanes-Macheteau, M., Rayon, C., Fischette-Lainé, A.-C., Gomord, V., & Faye, L. (1998). N-glycoprotein biosynthesis in plants: Recent developments and future trends. *Plant Molecular Biology, 38*(1), 31–48.

Lucas, P.-L., Mathieu-Rivet, E., Song, P. C. T., Oltmanns, A., Loutelier-Bourhis, C., Plasson, C., et al. (2020). Multiple xylosyltransferases heterogeneously xylosylate protein *N*-linked glycans in Chlamydomonas reinhardtii. *The Plant Journal, 102*(2), 230–245.

Määttänen, P., Gehring, K., Bergeron, J. J. M., & Thomas, D. Y. (2010). Protein quality control in the ER: The recognition of misfolded proteins. *Seminars in Cell & Developmental Biology, 21*(5), 500–511.

Manz, C., & Pagel, K. (2018). Glycan analysis by ion mobility-mass spectrometry and gas-phase spectroscopy. *Current Opinion in Chemical Biology, 42*, 16–24.

Mathieu-Rivet, E., Lerouge, P., & Bardor, M. (2017). *Chlamydomonas Reinhardtii*: Protein glycosylation and production of biopharmaceuticals. In M. Hippler (Ed.), *Chlamydomonas: Biotechnology and biomedicine* (pp. 45–72). Cham: M Springer International Publishing.

Matsui, T., Takita, E., Sato, T., Kinjo, S., Aizawa, M., Sugiura, Y., et al. (2011). N-glycosylation at non canonical Asn-X-Cys sequences in plant cells. *Glycobiology, 21*(8), 994–999.

May, J. C., Morris, C. B., & McLean, J. A. (2017). Ion mobility collision cross section compendium. *Analytical Chemistry, 89*(2), 1032–1044.

Mendes Siqueira, A. L., Beaumesnil, M., Hubert-Roux, M., Loutelier-Bourhis, C., Afonso, C., Bai, Y., et al. (2018). Atmospheric solid analysis probe coupled to ion mobility spectrometry-mass spectrometry, a fast and simple method for polyalphaolefin characterization. *Journal of the American Society for Mass Spectrometry, 29*(8), 1678–1687, 2018.

Mócsai, R., Blaukopf, M., Svehla, E., Kosma, P., & Altmann, F. (2020). The *N*-glycans of *Chlorella Sorokiniana* and a related strain contain arabinose but have strikingly different structures. *Glycobiology, 30*(8), 663–676.

Mócsai, R., Figl, R., Troschl, C., Strasser, R., Svehla, E., Windwarder, M., et al. (2019). N-glycans of the microalga *Chlorella Vulgaris* are of the oligomannosidic type but highly methylated. *Scientific Reports, 9*(1), 1–8.

Mohorko, E., Glockshuber, R., & Aebi, M. (2011). Oligosaccharyltransferase: The central enzyme of N-linked protein glycosylation. *Journal of Inherited Metabolic Disease, 34*(4), 869–878.

Pagel, K., & Harvey, D. J. (2013). Ion mobility–mass spectrometry of complex carbohydrates: Collision cross sections of sodiated N-linked glycans. *Analytical Chemistry, 85*(10), 5138–5145.

Plasencia, M. D., Isailovic, D., Merenbloom, S. I., Mechref, Y., & Clemmer, D. E. (2008). Resolving and assigning N-linked glycan structural isomers from ovalbumin by IMS-MS. *Journal of the American Society for Mass Spectrometry, 19*(11), 1706–1715.

Prien, J. M., Ashline, D. J., Lapadula, A. J., Zhang, H., & Reinhold, V. N. (2009). The high mannose glycans from bovine ribonuclease B isomer characterization by ion trap MS. *Journal of the American Society for Mass Spectrometry, 20*(4), 539–556.

Revercomb, H. E., & Mason, E. A. (1975). Theory of plasma chromatography/gaseous electrophoresis. *Analytical Chemistry, 47*, 970–983.

Rosales-Mendoza, S. (2016). Perspectives for the algae-made biopharmaceuticals Field. In S. Rosales-Mendoza (Ed.), *Algae-based biopharmaceuticals* (pp. 143–163). Cham: Springer International Publishing.

Rosales-Mendoza, S., Solís-Andrade, K. I., Márquez-Escobar, V. A., González-Ortega, O., & Bañuelos-Hernandez, B. (2020). Current advances in the algae-made biopharmaceuticals field. *Expert Opinion on Biological Therapy, 20*(7), 751–766.

Shi, X., & Jarvis, D. L. (2007). Protein N-glycosylation in the baculovirus-insect cell system. *Current Drug Targets, 8*(10), 1116–1125.

Smith, D. P., Knapman, T. W., Campuzano, I., Malham, R. W., Berryman, J. T., Radford, S. E., et al. (2009). Deciphering drift time measurements from travelling wave ion mobility spectrometry-mass spectrometry studies. *European Journal of Mass Spectrometry, 15*(2), 113–130.

Stanley, P., Taniguchi, N., & Aebi, M. (2015). N-glycans. In A. Varki, R. D. Cummings, J. D. Esko, P. Stanley, G. W. Hart, M. Aebi, … P. H. Seeberger (Eds.), *Essentials of glycobiology*. Cold Spring Harbor (NY): Cold Spring Harbor Laboratory Press.

Struwe, W. B., Pagel, K., Benesch, J. L. P., Harvey, D. J., & Campbell, M. P. (2016). GlycoMob: An ion mobility-mass spectrometry collision cross section database for glycomics. *Glycoconjugate Journal, 33*(3), 399–404.

Toraño, J. S., Aizpurua-Olaizola, O., Wei, N., Li, T., Unione, L., Jiménez-Osés, G., et al. (2020). Identification of isomeric *N*-glycans by conformer distribution fingerprinting using ion mobility-mass spectrometry. *Chemistry European Journal*. https://doi.org/10.1002/chem.202004522

Vanier, G., Hempel, F., Chan, P., Rodamer, M., Vaudry, D., Maier, U. G., et al. (2015). Biochemical characterization of human anti-hepatitis B monoclonal antibody produced in the microalgae *Phaeodactylum tricornutum*. *PloS One, 10*(10), Article 0139282.

Vanier, G., Lucas, P.-L., Loutelier-Bourhis, C., Vanier, J., Plasson, C., Walet-Balieu, M.-L., et al. (2017). Heterologous expression of the *N*-acetylglucosaminyltransferase I dictates a reinvestigation of the *N*-glycosylation pathway in *Chlamydomonas Reinhardtii*. *Scientific Reports, 7*(1), 1–12.

Vanier, G., Stelter, S., Vanier, J., Hempel, F., Maier, U. G., Lerouge, P., et al. (2018). Algae-made anti-hepatitis B antibody binds to human fcγ receptors. *Biotechnology Journal, 13*(4), Article 1700496.

Varki, A. (2017). Biological roles of glycans. *Glycobiology, 27*(1), 3–49.

Wildgoose, J. L., Giles, K., Pringle, S. D., Koeniger, S., Valentine, S. J., Bateman, R. H., et al. (2006). A comparison of travelling wave and drift tube ion mobility separations. *Proc. 54th ASMS Conference on Mass Spectrometry & Allied Topics*.

Zhang, P., Burel, C., Plasson, C., Kiefer-Meyer, M.-C., Ovide, C., Gügi, B., et al. (2019). Characterization of a GDP-fucose transporter and a fucosyltransferase involved in the fucosylation of glycoproteins in the diatom *Phaeodactylum tricornutum*. *Frontiers in Plant Science, 10*, 610.

Zhu, M., Bendiak, B., Clowers, B., & Hill, H. H. (2009). Ion mobility-mass spectrometry analysis of isomeric carbohydrate precursor ions. *Analytical and Bioanalytical Chemistry, 394*(7), 1853–1867.

Zhu, F., Lee, S., Valentine, S. J., Reilly, J. P., & Clemmer, D. E. (2012). Mannose7 glycan isomer characterization by IMS-MS/MS analysis. *Journal of the American Society for Mass Spectrometry, 23*(12), 2158–2166.